RGS6 and RGS7 Discriminate between the Highly Similar $G\alpha_i$ and $G\alpha_o$ Proteins Using a Two-Tiered Specificity Strategy

Ran Israeli, Ali Asli, Meirav Avital-Shacham and Mickey Kosloff

Department of Human Biology, *Faculty of Natural Sciences, University of Haifa, Haifa 3498838, Israel*

Correspondence to Mickey Kosloff: *Department of Human Biology, Faculty of Natural Sciences, University of Haifa, 199 Aba Khoushy Ave., Mt. Carmel, Haifa 3498838, Israel.* kosloff@sci.haifa.ac.il
https://doi.org/10.1016/j.jmb.2019.05.037
Edited by Igor Stagljar

Abstract

RGS6 and RGS7 are regulators of G protein signaling (RGS) proteins that inactivate heterotrimeric (αβγ) G proteins and mediate diverse biological functions, such as cardiac and neuronal signaling. Uniquely, both RGS6 and RGS7 can discriminate between $G\alpha_o$ and $G\alpha_{i1}$—two similar Gα subunits that belong to the same G_i sub-family. Here, we show that the isolated RGS domains of RGS6 and RGS7 are sufficient to achieve this specificity. We identified three specific RGS6/7 "disruptor residues" that can attenuate RGS interactions toward Gα subunits and demonstrated that their insertion into a representative high-activity RGS causes a significant, yet non-specific, reduction in activity. We further identified a unique "modulatory" residue that bypasses this negative effect, specifically toward $G\alpha_o$. Hence, the exquisite specificity of RGS6 and RGS7 toward closely related Gα subunits is achieved via a two-tier specificity system, whereby a Gα-specific modulatory motif overrides the inhibitory effect of non-specific disruptor residues. Our findings expand the understanding of the molecular toolkit used by the RGS family to achieve specific interactions with selected Gα subunits—emphasizing the functional importance of the RGS domain in determining the activity and selectivity of RGS R7 sub-family members toward particular Gα subunits.

Introduction

Heterotrimeric G proteins (αβγ) are molecular switches that regulate numerous intracellular signaling cascades, following their activation by G-protein coupled receptors [1,2]. The duration of G protein-coupled signaling is set by regulator of G protein signaling (RGS) proteins, which "turn off" activated Gα subunits [3,4]. This inactivation is mediated by the ~120-residue "RGS domain" found in all RGS proteins, where it functions as a GTPase activating protein (GAP) [5–7]. RGS proteins modulate numerous physiological functions and have been implicated in many human pathologies, making them promising drug targets [8–13]. In particular, RGS6 and RGS7, which belong to the R7 sub-family of RGS proteins, regulate diverse neuronal and cardiac circuits and signaling. RGS6 is predominantly expressed in the brain and heart and has been implicated in a variety of disorders [14], such as anxiety and depression [15], Parkinson's and Alzheimer's diseases [16,17], bradycardia [18], and cancer [19–21]. Likewise, RGS7 is mostly expressed in the brain and has been linked to many neurological disorders or functions, including anxiety [22], drug and reward behavior [23], multiple sclerosis [24], and synaptic plasticity [25]. However, how particular R7 sub-family members mediate individual biological functions and via which Gα subunits are not well understood.

A unique property of the R7 sub-family members RGS6 and RGS7 is their ability to discriminate between closely related Gα subunits, such as $G\alpha_o$ and $G\alpha_{i1}$ [26–28] (reviewed in Ref. [29]). In addition to the RGS domain, R7 sub-family proteins contain non-catalytic domains that mediate their sub-cellular localizations and interactions with additional proteins, such as the $G\beta_5$ subunit [30,31], which is essential for the stability of R7 sub-family members *in vivo* [32]. Two studies tested the activity of the full-length RGS6 and RGS7 proteins, which included these non-catalytic domains and observed higher

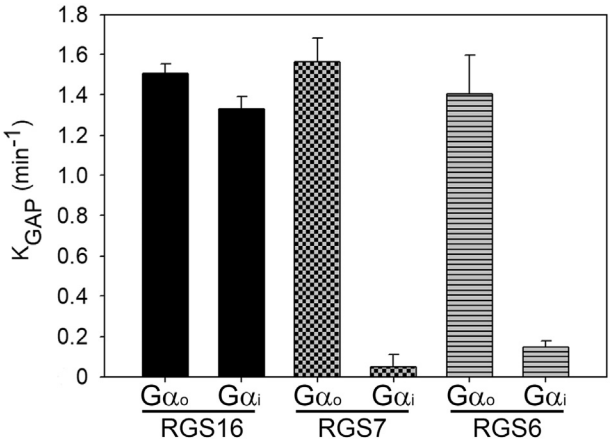

Fig. 1. The isolated RGS domains of RGS6 and RGS7 discriminate between $G\alpha_o$ and $G\alpha_{i1}$. GTPase rate constants were calculated using SigmaPlot 10.0 from single-exponential fits to the time course of GTP hydrolyzed by the Gα subunits (400 nM), with or without added RGS proteins (20 nM). k_{GAP} constants were calculated as in Ref. [43] by substracting the basal GTPase rate constant (i.e., without RGS protein) from the GTPase rate that was measured in the presence of the RGS protein. Values are means ± s.e.m. of $n \geq 3$ independent biological replicates.

GAP activity toward $G\alpha_o$ than toward $G\alpha_{i1}$ [26,28]. At the same time, others tested the activity of the isolated RGS7 domain and suggested that this domain is sufficient for mediating selectivity for $G\alpha_o$ over $G\alpha_{i1}$ [27]. As such, it remains unclear whether the RGS domains of RGS6 and RGS7 are sufficient for discriminating between $G\alpha_o$ and $G\alpha_{i1}$ or for achieving high GAP activity.

The particular structural features that might determine the specificities of R7 RGS sub-family members toward different Gα subunits have not been elucidated across the sub-family. Still, studies addressing this point have been conducted, but mostly focusing on the divergent RGS9. For instance, efforts have focused on the unique determinants that couple RGS9 and its specific affinity adaptor, the γ subunit of cGMP phosphodiesterase (PDEγ), to the visual G protein transducin ($G\alpha_t$) [33–37]. Skiba *et al.* [34] suggested that the Gα helical domain plays a role in mediating RGS9–PDEγ interaction specificity, while Sowa *et al.* [35] identified unique residues in the RGS9 domain responsible for specific interactions in the ternary complex that includes transducin and PDEγ. In this latter study, specific RGS7 residues, identified using the Evolutionary Trace method [38,39], were replaced with the corresponding RGS9 residues, resulting in an RGS7 domain that depended on PDEγ for high and specific GAP activity toward transducin. Here too, however, the structural determinants that modulated the specificity of RGS6 and RGS7 toward distinct Gα subunits were not elucidated.

Previously, we classified RGS residues into three groups, based on their mechanistic role in interactions with Gα subunits. The first group, termed "Significant & Conserved" residues, includes RGS residues that make similar and substantial contributions to interactions with Gα subunits across all high-activity RGS proteins [40]. The second group, "modulatory" residues, is composed of residues that contribute to interactions with Gα subunits only in some RGS proteins and were proposed to fine-tune specific G protein recognition [40,41]. The third group, "disruptor" residues, was recently identified and attenuates RGS activity for particular Gα subunits [41]. Three such disruptor residues in the R12 RGS sub-family were shown to reduce GAP activity toward $G\alpha_o$ via interactions with the Gα helical domain [41]. A partially overlapping set of disruptor residues were also identified in the RZ RGS sub-family [42]. Such classification has yet to be applied to the R7 sub-family. Moreover, neither modulatory nor disruptor residues have been identified in RGS6 and RGS7.

Here, we show that the isolated RGS domains of R7 sub-family members RGS6 and RGS7 are sufficient for discriminating between the highly similar $G\alpha_o$ and $G\alpha_{i1}$ proteins. Using sequence comparisons and structure-based modeling, we identified three putative R7 disruptor residues that can attenuate RGS6 and RGS7 GAP activity toward Gα subunits. Indeed, insertion of these residues into the high-activity RGS16 domain substantially reduced its GAP activity. Surprisingly, we found a unique structural motif that can bypass and override this disruption only toward $G\alpha_o$, namely, K428 in RGS7 and the homologous K431 in RGS6. We suggest that this lysine residue acts as a positive design element specifically toward $G\alpha_o$. We thus

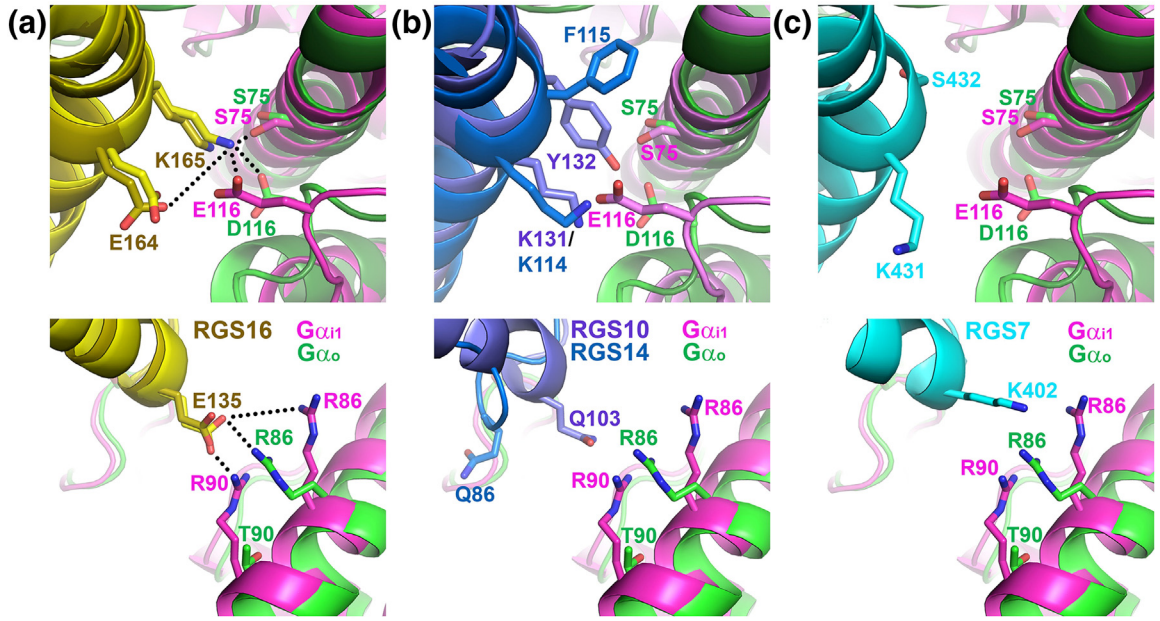

Fig. 2. Three RGS7 residues are comparable to R12 disruptor residues and are predicted to perturb favorable interactions with $G\alpha_o$ and $G\alpha_{i1}$. (a) Previously characterized R4 sub-family residues that contribute to favorable electrostatic interactions with the Gα helical domain, shown as sticks. Favorable salt bridges or hydrogen bonds are marked with dashed lines. RGS16–$G\alpha_{i1}$ and RGS16–$G\alpha_o$ complexes were superimposed and are shown as ribbon diagrams colored yellow/brown (RGS16 domains) and magenta/green ($G\alpha_{i1}$ and $G\alpha_o$). (b) The corresponding R12 disruptor residues shown to perturb interactions with $G\alpha_o$. RGS10 (purple) and RGS14 (blue) were superimposed onto the RGS16–$G\alpha_o$ and RGS16–$G\alpha_{i1}$ complexes, with Gα subunits colored as in a. (c) The corresponding RGS7 residues (K431 and S432, upper panel; K402, lower panel), modeled as in panel b.

propose a new two-tiered mechanism by which RGS proteins can discriminate between closely related Gα subunits.

Results

The RGS6 and RGS7 RGS domain discriminates between the highly similar $G\alpha_o$ and $G\alpha_{i1}$

We measured the GAP activity of representative R7 RGS domains toward the highly similar $G\alpha_o$ and $G\alpha_{i1}$ proteins, relative to the activity of RGS16. The latter is a representative of the R4 sub-family that was shown to have high activity toward $G\alpha_o$ and to similarly interact with $G\alpha_{i1}$ [40,41]. It should be noted that $G\alpha_o$ and $G\alpha_{i1}$ are 67% identical in sequence, and that their interfaces with RGS proteins are also quite similar, in that 27 of 32 Gα residues that are found ≤5 Å from the RGS domains in the $G\alpha_o$-RGS16 and $G\alpha_{i1}$-RGS16 structures are identical. We used single turnover GTPase assays with catalytic concentrations of RGS proteins to quantify the GAP activity of various RGS domains toward $G\alpha_o$ and $G\alpha_{i1}$ (Figs. 1 and S1). In contrast to RGS16, which, as expected, exhibited high GAP activity toward both $G\alpha_o$ and $G\alpha_{i1}$ (k_{GAP} = 1.5 and 1.4 min^{-1}, respectively), the RGS7 domain showed high GAP activity only toward $G\alpha_o$ (k_{GAP} = 1.6 min^{-1}), with only negligible activity toward $G\alpha_{i1}$ (k_{GAP} = 0.05 min^{-1}). RGS6, which is 81% identical in sequence to RGS7, also exhibited similar specificity, with k_{GAP} values of 1.4 min^{-1} toward $G\alpha_o$ and 0.15 min^{-1} toward $G\alpha_{i1}$ (Table S1).

Putative disruptor residues in RGS7 are predicted to interfere with its interactions with G_i sub-family members

We hypothesized that the basis for the discrimination between $G\alpha_o$ and $G\alpha_{i1}$ by RGS6 and RGS7 stems from residues that are unique to these RGS domains. To identify residues that might be responsible for the low GAP activity of RGS6 and RGS7 toward $G\alpha_{i1}$, we compared the sequences of the RGS domains from the R7 sub-family to the sequences of high-activity R4 sub-family members, and to the sequences of the previously investigated R12 sub-family [41]. Strikingly, the same three positions that were identified previously as disruptor residues in the R12 sub-family, which reduce RGS GAP activity, correspond to residues that are unique to RGS6 and RGS7 (Fig. S2).

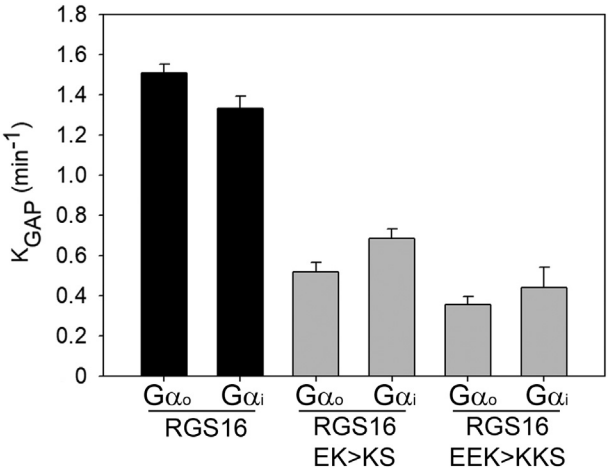

Fig. 3. Replacement of RGS16 modulatory residues that interact with the Gα helical domain with the corresponding RGS7 putative disruptor residues impairs GAP activity toward $G\alpha_o$ and $G\alpha_{i1}$. k_{GAP} constants for wild-type RGS16, and the E164K–K165S (EK > KS), and E135K–E164K–K165S (EEK > KKS) RGS16 mutants toward $G\alpha_o$ and $G\alpha_{i1}$. k_{GAP} constants were calculated as in Fig. 1. Values correspond to means ± s.e.m. from n ≥ 3 independent biological replicates.

Two of these positions correspond to RGS16 E164 and K165 (termed the "EK motif"), comprising a motif in high-activity RGS domains that interacts with residues on both sides of the RGS–Gα interface [41]. In particular, the EK motif forms an electrostatic/hydrogen bond network that includes both intramolecular and intermolecular interactions (Fig. 2a, upper panel). The third residue, RGS16 E135, forms a salt bridge with $G\alpha_o$ R86 or with $G\alpha_{i1}$ R86 and R90 (Fig. 2a, lower panel).

In contrast, the corresponding disruptor residues that were previously identified in the R12 sub-family [41] are predicted to attenuate inter-molecular interactions with Gα subunits (Fig. 2b). The R12 residues that correspond to the RGS16 EK motif, namely, K131–Y132 in RGS10 and K114–F115 in RGS14, cannot form the favorable electrostatic and hydrogen bond networks observed in high-activity RGS domains (Fig. 2b, upper panel). The third R12 residue, that is, Q103 in RGS10 and Q86 in RGS14, is also unable to form favorable interactions with Gα subunits (Fig. 2b, lower panel). Notably, a disruptor motif with a smaller effect was also described in the RZ RGS sub-family [42].

In modeling the interactions of RGS7 with $G\alpha_o$ and $G\alpha_{i1}$ (see Materials and Methods), we saw that RGS7 K431 and S432, which correspond to the RGS16 EK motif, are also predicted to perturb interactions with $G\alpha_o$ and $G\alpha_{i1}$ (Fig. 2c, upper panel), similarly to their R12 sub-family counterparts. Likewise, RGS7 K402, which corresponds to RGS16 E135, is also predicted to attenuate interactions with both Gα subunits (Fig. 2c, lower panel). The corresponding residues in RGS6 (H405, K434, and S435) are predicted to have a similar effect as their RGS7 counterparts (Fig. S3). This analysis thus pinpoints these three RGS7 residues as putative disruptor residues that can impair RGS GAP activity, similarly to their R12 counterparts.

Inserting the putative disruptor residues from RGS7 into RGS16 impairs GAP activity toward both $G\alpha_o$ and $G\alpha_{i1}$

To test the functional effect of these R7 putative disruptor residues, we inserted them into the high-activity RGS16 domain. We replaced the relevant RGS16 residues (E135, E164, K165) with their RGS7 counterparts and measured the GAP activities of the mutants using single turnover GTPase assays (Fig. 3). Substituting the RGS16 EK motif with the corresponding RGS7 residues (E164K and K165S, generating the RGS16 EK > KS mutant) substantially reduced GAP activity toward $G\alpha_o$ (k_{GAP} = 0.5 min^{-1}) and $G\alpha_{i1}$ (k_{GAP} = 0.7 min^{-1}). Additional substitution of the RGS16 E135 with its RGS7 lysine counterpart, generating the RGS16 EEK > KKS mutant, led to an additional small decrease in GAP activity toward both $G\alpha_o$ (k_{GAP} = 0.3 min^{-1}) and $G\alpha_{i1}$ (k_{GAP} = 0.5 min^{-1}). In contrast, mutating these motifs to alanines had no effect on GAP activity (Fig. S4a). Mutating residues adjacent to the EK motif (RGS16 Y168 and P169) to alanines also had no effect on GAP activity (Fig. S4b), as was also shown previously [41]. Lastly, substituting E135 and K165 with the corresponding serine and arginine residues from a divergent R4 RGS domain (RGS13) also had no effect on GAP activity (Fig. S4c). We therefore conclude that mutations in this region are not generally disruptive, as was also shown previously for the corresponding R12 positions [41], but rather that the presence of the specific R7 residues in these positions disrupts interactions with the Gα subunit and reduces GAP activity.

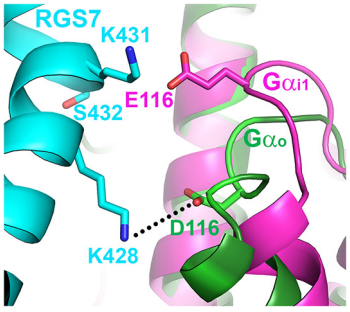

Fig. 4. RGS7 K428 can bypass the negative effect of the disruptor residues when interacting with $G\alpha_o$. RGS7 K428 is adjacent to $G\alpha_o$ D116 and can potentially form a salt bridge (marked with a dashed line) with this residue. The corresponding $G\alpha_{i1}$ E116 is too far to interact similarly with RGS7 K428. RGS7 complexes with $G\alpha_o$ and $G\alpha_{i1}$ were modeled as in Fig. 2, with RGS7 K431 and S432 shown for reference, rotated 90° about the *X*-axis relative to Fig. 2c.

A unique RGS6/7 lysine bypasses the negative effect of the R7 disruptor residues specifically toward $G\alpha_o$

Since the activity impairment caused by inserting the RGS7 putative disruptor residues into RGS16 was evident toward both $G\alpha_o$ and $G\alpha_{i1}$, this suggested that RGS7 contains a structural motif that can bypass the disruptor effect specifically toward $G\alpha_o$. We therefore examined the models of RGS7 complexed with $G\alpha_o$ and $G\alpha_{i1}$ to search for such a motif. We identified a particular lysine residue (RGS7 K428) that is unique to RGS6 and RGS7. This lysine residue is located close to the αB–αC loop of $G\alpha_o$, but is nevertheless too far to interact favorably with the αB–αC loop of $G\alpha_{i1}$ (Fig. 4). We therefore hypothesized that this putative interaction may underlie the high GAP activity of RGS7 seen specifically toward $G\alpha_o$. This interaction could involve formation of a favorable salt bridge only with $G\alpha_o$ D116 that could function as an alternative to the EK motif, but would not interact with the more distant $G\alpha_{i1}$ E116.

To test whether RGS7 K428 is indeed responsible for the selectivity of RGS7 toward $G\alpha_o$, we mutated this residue (marked as K*) to threonine, its RGS16 counterpart. Indeed, the GAP activity of the resulting RGS7 K*428T mutant toward $G\alpha_o$ was substantially reduced (k_{GAP} = 0.3 min^{-1}, Fig. 5a). In a reciprocal experiment, we substituted the corresponding threonine in RGS16 to a lysine, adding it to the background of the RGS16 EK > KS and RGS16 EEK > KKS mutants, yielding the RGS16 EK + T > KS + K* and RGS16 EEK + T- > KKS + K* mutants. This lysine substitution rescued the GAP activity of these mutants toward $G\alpha_o$, attaining similar GAP activity as wild-type RGS16 (k_{GAP} = 1.4 min^{-1} and k_{GAP} = 1.6 min^{-1}, correspondingly). This effect was specific for $G\alpha_o$, as this threonine-to-lysine substitution had no effect on the GAP activity of the RGS16 EK > KS mutant toward $G\alpha_{i1}$ (Fig. S5). To test whether the reciprocal mutants in RGS7 will relieve the disruption, we substituted the KS motif in RGS7 with the corresponding EK motif from RGS16, yielding the RGS7 KS > EK mutant. This substitution increased GAP activity to measurable levels (k_{GAP} = 0.3 min^{-1}, Fig. 5b), with the effect being

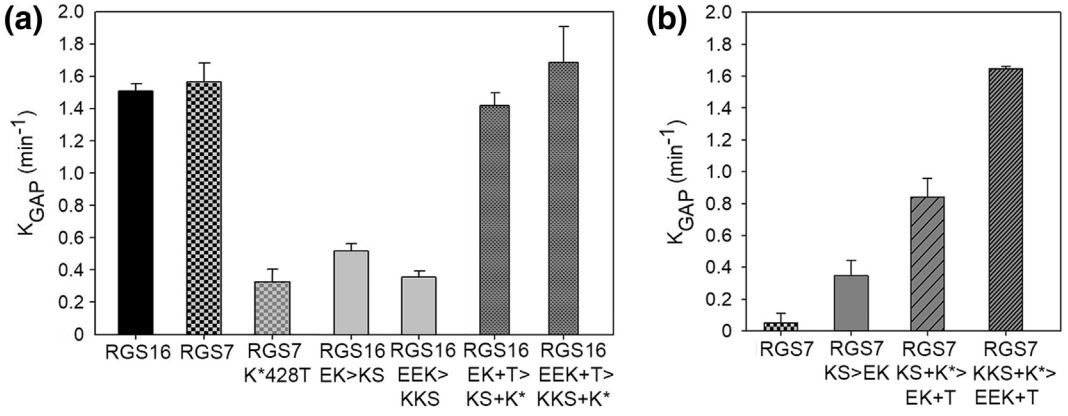

Fig. 5. A unique RGS6/7 modulatory lysine residue (K*) can selectively bypass the negative effect of the RGS7 disruptor residues. (a) k_{GAP} constants for RGS16 and RGS7 wild-type domains (taken from Fig. 1 for reference), RGS7 mutant K*428T and RGS16 mutants E164K–K165S (EK > KS), E135K–E164K–K165S (EEK > KKS), E164K–K165S–T131K* (EK + T > KS + K*), and E135K–E164K–K165S–T131K* (EEK + T > KKS + K*) toward $G\alpha_o$. K* denotes the unique modulatory RGS7 K428 residue (shown in Fig. 4) or a lysine residue inserted into the corresponding position in RGS16. (b) k_{GAP} constants for RGS7 wild-type (taken from Fig. 1 for reference) and the RGS7 mutants K431E–S432K (KS > EK), K431E–S432K–K*428T (KS + K* > EK + T), K402E–K431E–S432K–K*428T (KKS + K* > EEK + T) toward $G\alpha_{i1}$. k_{GAP} constants were calculated as in Fig. 1. Values correspond to means ± s.e.m. from n ≥ 3 independent biological replicates.

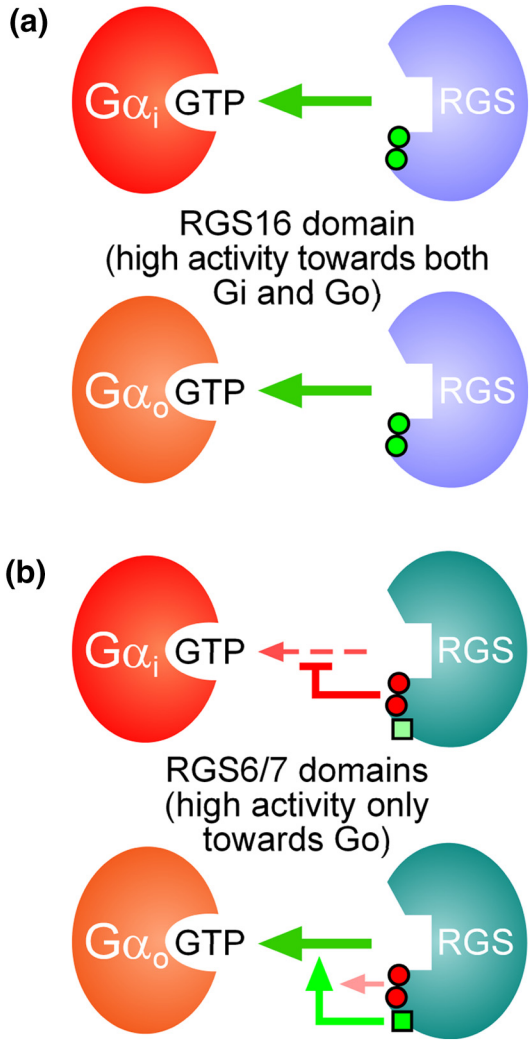

Fig. 6. Suggested molecular mechanism underlying the specificity of RGS6 and RGS7 toward $G\alpha_o$ and $G\alpha_{i1}$. (a) High-activity RGS domains such as RGS16 contain modulatory residues (green circles) that enable high GAP activity and do not discriminate between $G\alpha_o$ and $G\alpha_{i1}$. (b) RGS6 and RGS7 contain specific disruptor residues (red circles) that attenuate activity toward both $G\alpha_o$ and $G\alpha_{i1}$. RGS6/7 also contain a unique modulatory lysine residue (green square) that bypasses the inhibition of the disruptor residues selectively, only toward $G\alpha_o$, in a two-tiered specificity strategy.

specific for $G\alpha_{i1}$. Interestingly, substituting the unique RGS7 modulatory lysine with the corresponding threonine from RGS16 increased GAP activity further in the RGS7 KS + K^* > EK + T mutant (k_{GAP} = 0.8 min^{-1}). The complete substitution of all four of the RGS7-specific residues with their RGS16 counterparts, yielding the RGS7 KKS + K^* > EEK + T mutant, led to a full gain-of-function and maximal GAP activity toward $G\alpha_{i1}$ (k_{GAP} = 1.6 min^{-1}, Fig. 5b).

Discussion

Our results show that the RGS domains of RGS6 and RGS7 are sufficient for discriminating between $G\alpha_o$ and $G\alpha_i$—exhibiting high GAP activity toward $G\alpha_o$ and low GAP activity toward $G\alpha_{i1}$. Previous studies showed such selectivity with full-length RGS6 and RGS7 when co-expressed with $G\beta_5$, and suggested that the additional domains in these RGS proteins and/or $G\beta_5$ are the source of specificity [26,28]. On the other hand, an earlier study by Lan *et al.* [27] showed RGS7 specificity toward $G\alpha_o$ and $G\alpha_{i1}$ using the isolated RGS7 domain, measuring GTPase rates using a stopped-flow spectroscopic approach. Our results not only show that the isolated RGS domains of both RGS6 and RGS7 are sufficient for achieving $G\alpha_o/G\alpha_{i1}$ selectivity, but also demonstrate that the GAP activity of these isolated domains is highly similar to that of high-activity RGS domains from the R4 sub-family, such as RGS16.

We found that the RGS domains of both RGS6 and RGS7 contain three specific disruptor residues, which attenuate GAP activity toward $G\alpha_o$ and $G\alpha_{i1}$. Insertion of these residues into RGS16 revealed that the major inhibitory effect of these disruptor residues derives from the "KS motif" (residues 431–432 in RGS7), with only a minor additional effect that comes from RGS7 K402. The KS motif is identical in both RGS7 and RGS6, while RGS7 K402 corresponds to a histidine in RGS6 (Fig. S3). Previously, we showed that a histidine in the corresponding RGS18 position also contributed a minor inhibitory effect when inserted into RGS16 [41], leading to the prediction that the RGS6 disruptor residues should have the same effect as the RGS7 residues tested here. The direct effect of these RGS7 residues on RGS–Gα interactions differs from the mechanism that specifically couples RGS9 to $G\alpha_t$, which hinges on the specific recognition between RGS9 and PDEγ, with the latter functioning as an affinity adaptor [34–37].

Our results highlight a unique molecular mechanism by which the RGS6 and RGS7 domains achieve specificity toward $G\alpha_o$ over the closely related $G\alpha_i$ (Fig. 6). The R7-specific disruptor residues we identified here function via a similar mechanism as the disruptor residues that we identified in the R12 and RZ RGS subfamilies [41,42]—inhibiting GAP activity via intermolecular interactions with the Gα subunit. In the protein design field, such structural motifs have been termed "negative design elements," corresponding to structural elements that attenuate specific interactions between protein partners [44–46]. On the other hand, structural elements that enhance interactions between proteins partners were termed "positive design elements." Accordingly, the three R7 disruptor residues we identified here function as negative design elements. These R7 residues correspond to the three R12 subfamily disruptor residues identified previously [41], which are located at similar positions in the RGS

domain and were shown to underlie the lower GAP activity of the R12 sub-family. Both the R12 disruptor residues and the R7 residues we identified here interact similarly with the Gα helical domain. Moreover, the location of the R7 KS motif also corresponds to that of some of the disruptor residues identified in the RZ sub-family [42]. Comparable negative design elements were also shown to determine the discrimination of RGS2 between $G\alpha_{i1}$ and $G\alpha_q$, which also involves interactions with the Gα helical domain [47]. As such, the unfavorable inter-molecular interactions of negative design elements in RGS domains with the Gα helical domain emerges as a general mechanism that determines interaction specificity in all four RGS sub-families—the RZ, R4, R12, and R7 sub-families. On the other hand, our results pinpoint, for the first time, a unique positive design element in RGS6 and RGS7 that overrides the negative effect of the R7 disruptor residues in a specific fashion, only toward $G\alpha_o$ (Fig. 6). This selective positive design element combines with the non-selective disruptor residues in a two-tiered strategy to enable the exquisite specificity of these RGS proteins toward the highly similar $G\alpha_o$ and $G\alpha_i$ subunits.

In summary, our findings expand the understanding of the molecular toolkit used by the RGS family to achieve specific interactions with selected Gα subunits, involving a combination of specific negative design elements with a unique positive design element that bypasses the impact of the former in a selective manner. This emphasizes the functional importance of the RGS domain in determining the activity and selectivity of RGS R7 sub-family members toward particular Gα subunits. Nevertheless, the recently solved structure of the full-length RGS7 with $G\beta_5$ [48] showed that the additional domains of RGS7 and in particular the GGL domain, as well as $G\beta_5$, are adjacent to the RGS7 RGS domain and might therefore also contribute to interaction specificity allosterically (Fig. S6). Further studies using complementary methods such as molecular dynamic simulations will likely expand our understanding of such mechanisms. More generally, the design elements identified here enable R7 sub-family members to regulate diverse signaling pathways and suggest more specific avenues for studying their roles in such pathways. These, moreover, can serve to guide future drug design efforts targeting these interactions.

Materials and Methods

Protein structures and sequences

We used the following 3D structures in our visualization and analysis of RGS–Gα complexes, with Protein Data Bank (PDB) codes for each structure provided: human RGS16–$G\alpha_{i1}$ (PDB ID: 2IK8), mouse RGS16–$G\alpha_o$ (PDB ID: 3C7K), human RGS10–$G\alpha_{i3}$ (PDB ID: 2IHB), the monomeric NMR structure of human RGS14 (PDB ID: 2JNU), the x-ray crystal structure of the RGS domains of human RGS7 (PDB ID: 2A72) and RGS6 (PDB ID: 2ES0), and the structure of full-length RGS7 with $G\beta_5$ (PDB ID:6N9G). Because the RGS6 and RGS7 structures are atypical domain-swapped dimers in the x-ray structures, despite these proteins being monomers in solution [49], we modeled the monomeric forms of RGS6 and RGS7 bound to $G\alpha_o$ and $G\alpha_{i1}$ by superimposing each of the domain-swapped monomers onto RGS16 from the structure of RGS16–$G\alpha_o$ and splicing them together, with no additional perturbations to the structures. Missing atoms (in particular, RGS7 K402) were predicted using Scap [50]. Comparison to the recently solved structure of monomeric full-length RGS7 with $G\beta_5$ [48] showed that the positions of RGS7 side chains in the monomeric structure we used in our modeling were very similar to the conformations of the corresponding side chains in the full-length RGS7 structure. 3D structural visualizations and comparisons were carried out with the PyMOL molecular graphics program (http://pymol.org).

Protein expression, purification, and mutagenesi.

The human RGS6, RGS7, and RGS16 domains were expressed as N-terminally His_6-tagged fusion proteins using the pNIC-SGC1 (RGS6 and RGS7) and pLIC-SGC1 (RGS16) vectors (Addgene). $G\alpha_{i1}$ was expressed in the pProEXHTb vector (Invitrogen), while $G\alpha_o$ in the pT7–5 vector was a gift from Vadim Arshvashky (Duke University). RGS mutants were produced using the QuikChange Lightening site-directed mutagenesis kit (Invitrogen), with primers designed using the Primer Design Program (www.genomics.agilent.com). Proteins were expressed in *Escherichia coli* BL21 (DE3) cells and grown in 0.5 or 1 l of LB broth at 37 °C for RGS or Gα protein, respectively, until an OD_{600} (optical density at 600 nm) ≥ 1.4 was reached. The temperature was then reduced to 15 °C, and protein expression was induced by addition of 500 or 100 μM IPTG for RGS or Gα proteins, respectively. After 16–18 h, cells were harvested by centrifugation at 6000*g* for 30 min at 4 °C, followed by freezing the pellets at −80 °C. Pellets were re-suspended in lysis buffer [50 mM Tris–HCl (pH 8.0), 50 mM NaCl, 5 mM $MgCl_2$, 5 mM β-mercaptoethanol, protease inhibitor cocktail (Roche), and 0.5 mM phenylmethylsulfonyl fluoride (for G proteins only)], and the cells were lysed using a Sonics Vibra-Cell sonicator, followed by centrifugation at 24,000*g* for 30 min at 4 °C. The supernatants were equilibrated to 500 mM NaCl and 20 mM imidazole and loaded onto 1 ml HisTrap FF

columns (GE Healthcare Life Sciences). The columns were washed with >20 volumes of wash buffer [20 mM Tris–HCl (pH 8.0), 500 mM NaCl, 20 mM imidazole] at 4 °C and the tagged proteins were eluted with elution buffer [20 mM Tris–HCl (pH 8.0), 500 mM NaCl, 100 mM imidazole]. The eluate was loaded onto a HiLoad 16/600 Superdex 75 PG gel filtration column (GE Healthcare Life Sciences) at 4 °C with ≥1.5 volumes of GF elution buffer [50 mM Tris–HCl (pH 8.0), 50 mM NaCl, 5 mM β-mercaptoethanol, with 1 mM $MgCl_2$ added for Gα subunits only]. The eluate was dialyzed against dialysis buffer [GF elution buffer containing 40% (v/v) glycerol]. All purified proteins were estimated to be >95% pure, as assessed by SDS-polyacrylamide gel electrophoresis and Coomassie staining. Protein concentrations were determined by measuring absorption at 280 nm using predicted extinction coefficients (ProtParam, Swiss Institute for Bioinformatics) based on the sequence of each expressed protein.

Single-turnover GTPase assays

Single-turnover GTPase assays using $G\alpha_o$ or $G\alpha_{i1}$ and various RGS proteins (wild-type and mutants) were performed as described [40,41,43,51,52]. Briefly, Gα subunits in reaction buffer [50 mM Hepes (pH 7.5), 0.05% polyoxyethylene (v/v), 5 mM EDTA, 5 μg/ml bovine serum albumin, and 1 mM dithiothreitol] were incubated at 20 °C ($G\alpha_o$) or 30 °C ($G\alpha_{i1}$) for 15 min with 1 μM [γ-^{32}P]-GTP and cooled on ice for 5 min. GTP hydrolysis at 4 °C was initiated by increasing the magnesium concentration to 5 mM (with $MgCl_2$), together with 100 μM cold GTP (final concentration), with or without RGS proteins. Aliquots were removed at different time points and quenched on ice with 5% charcoal in 50 mM $Na_2H_2PO_4$ (pH 3), followed by centrifugation at 12,000*g* for 5 min at room temperature. Aliquots of the supernatants (200 μl) were added to 3 ml of scintillation liquid (PerkinElmer) and analyzed using a Tri-Carb 2810 TR scintillation counter (PerkinElmer). GTPase rates were determined from single-exponential fits to the GTPase time courses using SigmaPlot 10.0. k_{GAP} rate constants were determined by subtracting the basal GTPase rate (i.e., without RGS protein) from the GTPase rate that was measured in the presence of the RGS protein, as described [41,43].

CRediT author statement:

R.I. Conceptualization, Formal analysis, Investigation, Writing - original draft. **A.A.** Formal analysis, Methodology, Visualization, Writing - review & editing. **M.A.-S.** Methodology, Supervision, Resources, Writing - review & editing. **M.K.** Conceptualization, Formal analysis, Methodology, Investigation, Project administration, Supervision, Writing - original draft. All authors were involved in the writing of the manuscript and approved the final version.

Acknowledgments

We thank Liza Barki-Harrington for helpful comments. This work was supported by the Israel Science Foundation (grants 1454/13, 1959/13, and 2155/15).

Declaration of Interests: The authors declare that they have no competing interests.

Appendix A. Supplementary data

Supplementary data to this article can be found online at https://doi.org/10.1016/j.jmb.2019.05.037.

Received 30 January 2019;
Received in revised form 12 May 2019;
Available online 30 May 2019

Keywords:
G protein signaling;
interaction specificity;
PPI;
protein structure;
RGS proteins

Abbreviations used:
RGS, Regulator G protein signaling; GAP, GTPase activating protein; PDB, Protein Data Bank.

References

[1] S.R. Sprang, G protein mechanisms: insights from structural analysis, Annu. Rev. Biochem. 66 (1997) 639–678.
[2] W.M. Oldham, H.E. Hamm, Heterotrimeric G protein activation by G-protein-coupled receptors, Nat. Rev. Mol. Cell Biol. 9 (2008) 60–71.
[3] M.R. Koelle, H.R. Horvitz, EGL-10 regulates G protein signaling in the C. elegans nervous system and shares a conserved domain with many mammalian proteins, Cell. 84 (1996) 115–125.
[4] D.P. Siderovski, A. Hessel, S. Chung, T.W. Mak, M. Tyers, A new family of regulators of G-protein-coupled receptors? Current biology : CB. 6 (1996) 211–212.
[5] D.M. Berman, T.M. Wilkie, A.G. Gilman, GAIP and RGS4 are GTPase-activating proteins for the Gi subfamily of G protein alpha subunits, Cell. 86 (1996) 445–452.
[6] T.W. Hunt, T.A. Fields, P.J. Casey, E.G. Peralta, RGS10 is a selective activator of G alpha i GTPase activity, Nature. 383 (1996) 175–177.

[7] N. Watson, M.E. Linder, K.M. Druey, J.H. Kehrl, K.J. Blumer, RGS family members: GTPase-activating proteins for heterotrimeric G-protein alpha-subunits, Nature. 383 (1996) 172–175.
[8] S. Hollinger, J.R. Hepler, Cellular regulation of RGS proteins: modulators and integrators of G protein signaling, Pharmacol. Rev. 54 (2002) 527–559.
[9] R.R. Neubig, Regulators of G protein signaling (RGS proteins): novel central nervous system drug targets, J. Pept. Res. 60 (2002) 312–316.
[10] K.L. Neitzel, J.R. Hepler, Cellular mechanisms that determine selective RGS protein regulation of G protein-coupled receptor signaling, Semin. Cell Dev. Biol. 17 (2006) 383–389.
[11] J.H. Hurst, S.B. Hooks, Regulator of G-protein signaling (RGS) proteins in cancer biology, Biochem. Pharmacol. 78 (2009) 1289–1297.
[12] A.J. Kimple, D.E. Bosch, P.M. Giguere, D.P. Siderovski, Regulators of G-protein signaling and their Galpha substrates: promises and challenges in their use as drug discovery targets, Pharmacol. Rev. 63 (2011) 728–749.
[13] B. Sjogren, Regulator of G protein signaling proteins as drug targets: current state and future possibilities, Adv. Pharmacol. 62 (2011) 315–347.
[14] K.E. Squires, C. Montanez-Miranda, R.R. Pandya, M.P. Torres, J.R. Hepler, Genetic analysis of rare human variants of regulators of G protein signaling proteins and their role in human physiology and disease, Pharmacol. Rev. 70 (2018) 446–474.
[15] A. Stewart, B. Maity, A.M. Wunsch, F. Meng, Q. Wu, J.A. Wemmie, et al., Regulator of G-protein signaling 6 (RGS6) promotes anxiety and depression by attenuating serotonin-mediated activation of the 5-HT(1A) receptor-adenylyl cyclase axis, FASEB journal. 28 (2014) 1735–1744.
[16] P. Bifsha, J. Yang, R.A. Fisher, J. Drouin, RGS6 is required for adult maintenance of dopaminergic neurons in the ventral substantia nigra, PLoS Genet. 10 (2014), e1004863.
[17] S.W. Moon, I.D. Dinov, J. Kim, A. Zamanyan, S. Hobel, P.M. Thompson, et al., Structural neuroimaging genetics interactions in Alzheimer's disease, Journal of Alzheimer's disease : JAD. 48 (2015) 1051–1063.
[18] J. Yang, J. Huang, B. Maity, Z. Gao, R.A. Lorca, H. Gudmundsson, et al., RGS6, a modulator of parasympathetic activation in heart, Circ. Res. 107 (2010) 1345–1349.
[19] D.M. Berman, Y. Wang, Z. Liu, Q. Dong, L.A. Burke, L.A. Liotta, et al., A functional polymorphism in RGS6 modulates the risk of bladder cancer, Cancer Res. 64 (2004) 6820–6826.
[20] J. Yang, L.T. Platt, B. Maity, K.E. Ahlers, Z. Luo, Z. Lin, et al., RGS6 is an essential tumor suppressor that prevents bladder carcinogenesis by promoting p53 activation and DNMT1 downregulation, Oncotarget. 7 (2016) 69159–69172.
[21] K.E. Ahlers, B. Chakravarti, R.A. Fisher, RGS6 as a novel therapeutic target in CNS diseases and cancer, AAPS J. 18 (2016) 560–572.
[22] C. Hohoff, A. Neumann, K. Domschke, C. Jacob, W. Maier, J. Fritze, et al., Association analysis of RGS7 variants with panic disorder, J. Neural Transm. 116 (2009) 1523–1528.
[23] L.P. Sutton, O. Ostrovskaya, M. Dao, K. Xie, C. Orlandi, R. Smith, et al., Regulator of G-protein signaling 7 regulates reward behavior by controlling opioid signaling in the striatum, Biol. Psychiatry 80 (2016) 235–245.
[24] J.L. McCauley, R.L. Zuvich, Y. Bradford, S.J. Kenealy, N. Schnetz-Boutaud, S.G. Gregory, et al., Follow-up examination of linkage and association to chromosome 1q43 in multiple sclerosis, Genes Immun. 10 (2009) 624–630.
[25] O. Ostrovskaya, K. Xie, I. Masuho, A. Fajardo-Serrano, R. Lujan, K. Wickman, et al., RGS7/Gbeta5/R7BP complex regulates synaptic plasticity and memory by modulating hippocampal GABABR-GIRK signaling, eLife. 3 (2014), e02053.
[26] B.A. Posner, A.G. Gilman, B.A. Harris, Regulators of G protein signaling 6 and 7. Purification of complexes with Gbeta5 and assessment of their effects on G protein-mediated signaling pathways, J. Biol. Chem. 274 (1999) 31087–31093.
[27] K.L. Lan, H. Zhong, M. Nanamori, R.R. Neubig, Rapid kinetics of regulator of G-protein signaling (RGS)-mediated G-alpha-i and G-alpha-o deactivation. G-alpha specificity of RGS4 and RGS7, J. Biol. Chem. 275 (2000) 33497–33503.
[28] S.B. Hooks, G.L. Waldo, J. Corbitt, E.T. Bodor, A.M. Krumins, T.K. Harden, RGS6, RGS7, RGS9, and RGS11 stimulate GTPase activity of Gi family G-proteins with differential selectivity and maximal activity, J. Biol. Chem. 278 (2003) 10087–10093.
[29] B. Sjogren, L.L. Blazer, R.R. Neubig, Regulators of G protein signaling proteins as targets for drug discovery, Progress in Molecular Biology and Translational Science vol. 91 (2010) 81–119.
[30] E.R. Makino, J.W. Handy, T. Li, V.Y. Arshavsky, The GTPase activating factor for transducin in rod photoreceptors is the complex between RGS9 and type 5 G protein beta subunit, Proc. Natl. Acad. Sci. U. S. A. 96 (1999) 1947–1952.
[31] D.S. Witherow, Q. Wang, K. Levay, J.L. Cabrera, J. Chen, G. B. Willars, et al., Complexes of the G protein subunit Gbeta 5 with the regulators of G protein signaling RGS7 and RGS9. Characterization in native tissues and in transfected cells, J. Biol. Chem. 275 (2000) 24872–24880.
[32] C.K. Chen, P. Eversole-Cire, H. Zhang, V. Mancino, Y.J. Chen, W. He, et al., Instability of GGL domain-containing RGS proteins in mice lacking the G protein beta-subunit Gbeta5, Proc. Natl. Acad. Sci. U. S. A. 100 (2003) 6604–6609.
[33] W. He, C.W. Cowan, T.G. Wensel, RGS9, a GTPase accelerator for phototransduction, Neuron. 20 (1998) 95–102.
[34] N.P. Skiba, C.S. Yang, T. Huang, H. Bae, H.E. Hamm, The alpha-helical domain of G-alpha-t determines specific interaction with regulator of G protein signaling 9, J. Biol. Chem. 274 (1999) 8770–8778.
[35] M.E. Sowa, W. He, K.C. Slep, M.A. Kercher, O. Lichtarge, T. G. Wensel, Prediction and confirmation of a site critical for effector regulation of RGS domain activity, Nat. Struct. Biol. 8 (2001) 234–237.
[36] K.C. Slep, M.A. Kercher, W. He, C.W. Cowan, T.G. Wensel, P.B. Sigler, Structural determinants for regulation of phosphodiesterase by a G protein at 2.0 A, Nature. 409 (2001) 1071–1077.
[37] K.A. Martemyanov, V.Y. Arshavsky, Noncatalytic domains of RGS9-1.Gbeta 5L play a decisive role in establishing its substrate specificity, J. Biol. Chem. 277 (2002) 32843–32848.
[38] O. Lichtarge, H.R. Bourne, F.E. Cohen, Evolutionarily conserved G-alpha-beta-gamma binding surfaces support a model of the G protein-receptor complex, Proc. Natl. Acad. Sci. U. S. A. 93 (1996) 7507–7511.
[39] O. Lichtarge, H.R. Bourne, F.E. Cohen, An evolutionary trace method defines binding surfaces common to protein families, J. Mol. Biol. 257 (1996) 342–358.
[40] M. Kosloff, A.M. Travis, D.E. Bosch, D.P. Siderovski, V.Y. Arshavsky, Integrating energy calculations with functional

assays to decipher the specificity of G protein–RGS protein interactions, Nat. Struct. Mol. Biol. 18 (2011) 846–853.
[41] A. Asli, I. Sadiya, M. Avital-Shacham, M. Kosloff, "Disruptor" residues in the regulator of G protein signaling (RGS) R12 subfamily attenuate the inactivation of Galpha subunits, Sci. Signal. 11 (2018).
[42] D. Salem-Mansour, A. Asli, M. Avital-Shacham, M. Kosloff, Structural motifs in the RGS RZ subfamily combine to attenuate interactions with Galpha subunits, Biochem. Biophys. Res. Commun. 503 (2018) 2736–2741.
[43] E.M. Ross, Quantitative assays for GTPase-activating proteins, Methods Enzymol. 344 (2002) 601–617.
[44] M.H. Hecht, J.S. Richardson, D.C. Richardson, R.C. Ogden, De novo design, expression, and characterization of Felix: a four-helix bundle protein of native-like sequence, Science. 249 (1990) 884–891.
[45] J.J. Havranek, Specificity in computational protein design, J. Biol. Chem. 285 (2010) 31095–31099.
[46] G. Schreiber, A.E. Keating, Protein binding specificity versus promiscuity, Curr. Opin. Struct. Biol. 21 (2011) 50–61.
[47] M. Kasom, S. Gharra, I. Sadiya, M. Avital-Shacham, M. Kosloff, Interplay between negative and positive design elements in Galpha helical domains of G proteins determines interaction specificity toward RGS2, The Biochemical journal. 475 (2018) 2293–2304.
[48] D.N. Patil, E.S. Rangarajan, S.J. Novick, B.D. Pascal, D.J. Kojetin, P.R. Griffin, et al., Structural organization of a major neuronal G protein regulator, the RGS7–Gbeta5–R7BP complex, eLife. 7 (2018).
[49] M. Soundararajan, F.S. Willard, A.J. Kimple, A.P. Turnbull, L. J. Ball, G.A. Schoch, et al., Structural diversity in the RGS domain and its interaction with heterotrimeric G protein alpha-subunits, Proc. Natl. Acad. Sci. U. S. A. 105 (2008) 6457–6462.
[50] Z. Xiang, B. Honig, Extending the accuracy limits of prediction for side-chain conformations, J. Mol. Biol. 311 (2001) 421–430.
[51] J. Wang, Y. Tu, J. Woodson, X. Song, E.M. Ross, A GTPase-activating protein for the G protein G-alpha-z. Identification, purification, and mechanism of action, J. Biol. Chem. 272 (1997) 5732–5740.
[52] B.A. Posner, S. Mukhopadhyay, J.J. Tesmer, A.G. Gilman, E. M. Ross, Modulation of the affinity and selectivity of RGS protein interaction with G alpha subunits by a conserved asparagine/serine residue, Biochemistry. 38 (1999) 7773–7779.